Published in final edited form as:
Cancer Cell. 2008 December 9; 14(6): 447–457. doi:10.1016/j.ccr.2008.10.018.

Distinct thresholds govern Myc's biological output *in vivo*

J. Murphy Daniel[1,+,$], **Melissa R. Junttila**[1,*,$], **Laurent Pouyet**[1], **Anthony Karnezis**[2], **Ksenya Shchors**[1], **Duyen A. Bui**[1,@], **Lamorna Brown-Swigart**[1], **Leisa Johnson**[3], and **Gerard. I. Evan**[1,2,#]

[1] University of California San Francisco, Dept. of Pathology

[2] University of California San Francisco, Helen Diller Family Comprehensive Cancer Center

[3] Genentech Inc., South San Francisco

[*] Enrique Cepero, PhD Fellow of the Damon Runyon Cancer Research Foundation

SUMMARY

Deregulated Myc triggers a variety of intrinsic tumor suppressor programs that serve to restrain Myc's oncogenic potential. Since Myc activity is also required for normal cell proliferation, activation of intrinsic tumor suppression must be triggered only when Myc signaling is oncogenic. However, how cells discriminate between normal and oncogenic Myc is unknown. Here we show that distinct threshold levels of Myc govern its output *in vivo*: low levels of deregulated Myc are competent to drive ectopic proliferation of somatic cells and oncogenesis but activation of the apoptotic and ARF/p53 intrinsic tumor surveillance pathways requires Myc over-expression. The requirement to keep activated oncogenes at low level to avoid engaging tumor suppression is likely an important selective pressure governing the early stages of tumor microevolution.

SIGNIFICANCE

Cancers are prevented by the activation of intrinsic tumor suppression programs that either fix the damage in cells or ensure that the damaged cells cannot propagate. Cancers can only arise once these tumor suppressor pathways are abrogated. Importantly, activation of such tumor suppressor pathways must be restricted only by oncogenic, not normal, growth signals. Using a novel *in vivo* model of Myc-induced tumorigenesis in which Myc function is deregulated without concomitant over-expression, we show that tumor surveillance programs are triggered specifically by Myc over-expression, not deregulation. Nonetheless, low-level deregulated Myc remains potently oncogenic. These observations identify a novel mechanism by which the tumor suppressor defense mechanisms can be circumvented, with implications for our understanding of early stage neoplasia.

INTRODUCTION

The Myc oncoprotein is a pleiotropic transcription factor of the bHLH-LZip family with the essential role of engaging and coordinating expression of the diverse genes necessary for

#To whom correspondence should be addressed: gevan@cc.ucsf.edu (+1 415 514 9760).
[+]Present address: Lehrstuhl fuer Physiogolische Chemie II, Am Hubland, 97074 Wuerzburg, Germany
[@]Present address: Department of Cell Biology, 240 Longwood Avenue, Building C1, Room 513B, Harvard Medical School, Boston, MA 02115
[$]These authors contributed equally

efficient and orderly proliferation of somatic cells. In normal cells, both c-Myc mRNA and protein expression are low and continuously dependent on mitogen signaling (Liu and Levens, 2006; Rabbitts *et al*., 1985; Ramsay *et al*., 1984). In most human cancers, by contrast, Myc expression is deregulated and/or elevated. Sometimes this is due to alterations in the *myc* gene itself that either disrupt its normal regulation (e.g. chromosomal translocation, retrovirus integration, gene amplification), increase Myc mRNA or protein stability, or abrogate Myc auto-repression (reviewed by (Nesbit *et al*., 1999; Popescu and Zimonjic, 2002; Spencer and Groudine, 1991). In most tumors, however, the c-*myc* gene appears normal and its elevated and persistent activity appears to be due to its relentless induction by upstream oncoproteins, such as oncogenic kinases, Ras or the Wnt/β-Catenin pathway.

The extent to which Myc deregulation versus Myc over-expression contributes to Myc oncogenic activity is unclear. Increasing Myc levels often correlate with the more advanced and aggressive variants of tumors, suggesting that over-expression plays some part in Myc-driven oncogenesis. Moreover, since over-expression drives novel interactions between Myc and low affinity promoter elements, some have suggested that Myc's oncogenic actions arise from precocious recruitment of novel genes (Fernandez *et al*., 2003). On the other hand, deregulation of Myc without over-expression is sufficient to obviate the dependency of normal cell proliferation on mitogens and to block the response of cycling cells to anti-proliferative cues and is most likely a consequence of aberrantly sustained modulation of normal Myc target genes.

It is now generally accepted that spontaneous tumorigenesis is largely suppressed by the obligate coupling of proliferation to anti-oncogenic programs such as senescence and apoptosis (Evan and Littlewood, 1998; Lowe *et al.*, 2004). Myc is a prototypical example of this phenomenon. Oncogenically activated Myc is a potent inducer of cell proliferation but also engages the ARF/p53 tumor suppressor pathway (Eischen *et al.*, 1999; Kamijo *et al.*, 1998; Schmitt *et al.*, 1999; Zindy *et al.*, 1998) and apoptosis (Askew *et al*., 1991; Evan *et al*., 1992), both tumor suppressor programs that antagonize cell expansion and restrict Myc's oncogenic potential. However, since Myc mediates the proliferation of normal cells, it is clear that activation of ARF/p53 and apoptosis must be restricted to situations where Myc is oncogenic. How cells distinguish between Myc that is activated by mitogenic signals and Myc that is oncogenically activated is unknown, although candidates include the abnormal persistence of oncogenic Myc, its activation outside the normal context of other mitogenic signals, and its over-expression.

To address these issues, we have developed a novel Myc transgenic mouse in which latent expression of the reversibly switchable variant of Myc, MycER^{T2} is driven by the constitutive and ubiquitously active *Rosa26* promoter. Overt MycER^{T2} expression is then triggered in any target tissue by the hit-and-run action of Cre recombinase. Due to the relative weakness of the *Rosa26* promoter, the level of MycER expressed in tissues of such animals is very low and close to the physiological level of Myc following normal mitogen stimulation. We have used this model to define the oncogenic properties of Myc *in vivo* when deregulated but not significantly over-expressed. Our studies indicate that the level at which Myc is expressed plays an unforeseen and critical role in determining its oncogenic potential.

RESULTS

Generation of *R26-lsl-MER^{T2}* and *R26-MER^{T2}* mice

The switchable, 4-hydroxytamoxifen (4-OHT)-dependent variant of Myc was generated by fusing Myc to the modified hormone-binding domain of the modified estrogen receptor ER^{T2} (Indra *et al*., 1999). To direct expression conditionally of MycER^{T2} to target tissues, the cDNA was inserted downstream of the ubiquitously active *Rosa26* locus, preceded by a strong

translational termination sequence flanked by *loxP* recombination sites. Murine embryonic stem (ES) cell clones transfected with the resulting targeting vector were screened by Southern blotting to identify single insertions into the *Rosa26* locus (Supplemental Fig. 1). Germ line transmission of the *R26-lsl-MER^{T2}* allele by chimeric mice was verified by PCR amplification across the Myc-ER^{T2} sequence junction. We refer to the resulting line of mice as *R26-lsl-MER^{T2}*.

To verify that MycER^{T2} expression is dependent upon excision of the translational termination element, we expressed Cre recombinase in *R26-lsl-MycER^{T2}*-derived embryonic fibroblasts (MEFs). Immunoblotting with anti-human ER antibody demonstrated expression of the predicted 92 kDa MycER^{T2} fusion protein only in MEFs expressing Cre (Fig. 1A). To compare directly in somatic cells and tissues the levels of *MycER^{T2}* expression driven from one or two copies of the *Rosa26* promoter with those of endogenous Myc, *R26-lsl-MycER^{T2}* mice were crossed with the germ line deletor strain, *ZP3-Cre* (Lewandoski *et al.*, 1997). *Rosa26*-driven MycER^{T2} is expressed in all somatic cells of such crosses, which we henceforth refer to as *R26^{MER}* mice. Relative levels of endogenous Myc and ectopic MycER^{T2} proteins in log phase, serum-deprived and serum-stimulated WT MEFs, and in heterozygous *R26$^{MER/WT}$* and homozygous *R26$^{MER/MER}$* MEFs were then compared by immunoblotting cell extracts with SC42 anti-Myc antibody, which recognizes an epitope common to Myc and MycER^{T2}. MycER^{T2}, absent from WT MEFs, was expressed in homozygous *R26$^{MER/MER}$* cells at approximately twice the level of MycER^{T2} present in heterozygous *R26$^{MER/WT}$* cells (Figure 1B). This was confirmed at the mRNA level by real–time quantitative PCR (Figure 1C). The steady state level of MycER^{T2} in *R26$^{MER/WT}$* MEFs was a little below, and the MycER^{T2} levels in *R26$^{MER/MER}$* MEFs a little above, that of endogenous Myc in logarithmically growing WT MEFs, and far below the ~30,000 Myc molecules per cell present in HeLa cells (Moore *et al.*, 1987). MycER^{T2} protein half-life was short (15–20′) (Suppl. Fig. 2A), essentially identical to that of endogenous Myc (Flinn *et al.*, 1998;Ramsay *et al.*, 1984). Unlike endogenous Myc, however, *R26*-driven MycER^{T2} expression was unaffected by serum status (Suppl. Fig. 2B). Above ~10,000 total Myc molecules per cell, Myc autoregulates, suppressing expression from its endogenous promoter (Penn et al., 1990). To ascertain whether MycER^{T2}, when activated, is expressed at a level sufficient to suppress endogenous Myc, we repeated the analysis in Figure 1B using MEFs treated continuously with 4-OHT to activate MycER^{T2}. We observed negligible down-regulation of endogenous Myc upon activation of MycER^{T2} in either *R26$^{MER/wt}$* or *R26$^{MER/MER}$* MEFs (Suppl. Fig. 2C), consistent with the very low levels of MycER^{T2} present in *R26^{MER}* MEFs.

We used Q-PCR with selective primers both to quantitate the relative levels of endogenous *myc* versus *MycER^{T2}* mRNA in tissues of tamoxifen-treated and untreated *R26$^{MER/MER}$* mice and to assess whether endogenous Myc expression is suppressed by *R26*-driven MycER^{T2} *in vivo*. As expected, levels of endogenous Myc were extremely low in non-proliferating tissues. In spleen, where cell proliferation is substantial, MycER^{T2} mRNA levels were comparable with those of endogenous *myc*. We observed no significant suppression of endogenous Myc upon activation of MycER^{T2} in any tissue aside from colonic epithelium (Suppl. Fig. 3).

Deregulated expression of low-level Myc induces ectopic proliferation in multiple adult tissues

The relative contributions to oncogenesis made by Myc deregulation versus Myc over-expression remain unclear. The low level of deregulated MycER^{T2} expression in *R26^{MER}* tissues therefore provided a unique opportunity to ascertain the impact of Myc deregulation, without overt over-expression, in adult mouse tissues. To confirm *MycER^{T2}* expression in tissues, RNA was extracted from multiple organs from adult (2-month old) homozygous *R26-lsl-MER^{T2}* and hetero *R26$^{MER/wt}$* and *R26$^{MER/MER}$* homozygous mice and *MycER^{T2}* transcript

levels quantified by Q-PCR. *MycER^{T2}* mRNA was essentially undetectable in any organs of *R26-lsl-MycER^{T2}* mice but exhibited gene dose-dependent expression in all tested organs of *R26^{MER}* animals (Fig. 2A).

To activate MycER^{T2} acutely in all tissues, tamoxifen was daily administered systemically for 6 days to adult *R26$^{WT/WT}$*, *R26$^{MER/}$*^{WT} and *R26$^{MER/MER}$* mice. Proliferation in tissues was assessed by systemic administration of BrdU at day 3 followed by iododeoxyuridine (IdU) at day 6 to capture initial and delayed S phases (Burns and Kuan, 2005). BrdU and IdU incorporation in most tissues of tamoxifen-treated *R26$^{MER/WT}$* (colonic epithelium was the exception – see below) was indistinguishable from that in *R26$^{WT/WT}$*; by contrast, we saw a marked increase in incorporation of both BrdU and IdU in multiple tissues of homozygous *R26$^{MER/MER}$* animals (Fig. 2B) - including exocrine pancreas, endocrine pancreas, kidney, liver and lung. Of note, no proliferation was observed in skeletal or cardiac muscle, or in brain aside from the epithelial choroid plexus (Suppl. Table 1). These data demonstrate that deregulation of low-level Myc is alone sufficient to drive sustained proliferation in a significant subset of tissues. However, MycER^{T2}-induced proliferation was only evident in homozygous *R26$^{MER/MER}$* tissues (Fig. 2C), indicating that a critical minimum threshold level of Myc is needed to drive proliferation in "permissive" tissues and this threshold is straddled by the levels of MycER^{T2} expression in hetero- and homozygous *Rosa26-MycER^{T2}* mice. *Ipso facto*, we conclude that the ectopic Myc activity in tissues of homozygous *R26$^{MER/MER}$* mice is close to the minimum required to drive ectopic proliferation.

Different threshold levels of Myc trigger Myc-induced proliferation versus induction of apoptosis and *ARF*

Myc-induced apoptosis is a key intrinsic tumor suppressor mechanism that limits Myc oncogenic potential. However, which factors determine whether proliferation or cell death is the predominant outcome of Myc activation remain unclear. To ascertain whether activation of low-level MycER^{T2} induces apoptosis in tissues *in vivo*, Myc was activated systemically in adult *R26$^{MER/MER}$* mice for 0, 3 or 6 days and tissue sections from multiple organs then probed with Ki67-specific antibody to identify cells in cycle, and by TUNEL to identify apoptotic cells. As with our BrdU/IdU incorporation data, proliferation was robustly induced by 3 days of MycER^{T2} activation in the same proliferation permissive organs as above, remaining elevated at 6 days in pancreatic islets, kidney and lung (Fig. 3A and Suppl. Fig. 4; summarized in Suppl. Table 1). However, we observed no Myc-induced apoptosis in any tissues (with the exception of colonic epithelium - see below). We conclude that quasi-physiological levels of deregulated Myc are sufficient to drive proliferation in most permissive tissues without engaging concomitant apoptosis.

As mentioned, colonic epithelium of *R26$^{MER/MER}$* mice was a notable exception to the above: Myc activation induced abundant apoptosis. Provocatively, out of all *R26^{MER}* tissues tested, colonic epithelium exhibited the highest level of MycER^{T2} expression (Fig. 2A). Indeed, even the single allele of *MycER^{T2}* in heterozygous *R26$^{MER/WT}$* mice drove sufficient Myc expression to trigger proliferation in colonic epithelium upon activation (P value = 0.001; Fig. 3B). In colonic epithelium of homozygous *R26$^{MER/MER}$* animals (Fig. 3B) Myc-induced proliferation was even more marked: although accompanied by apoptosis (Fig. 3C). Together, these observations intimated that induction of apoptosis *in vivo* might require a higher level of Myc than proliferation.

Like apoptosis, induction of p19^{ARF} by oncogenic Myc is a critical restraint to Myc oncogenesis that, by activating p53 through inhibition of Mdm-2 (Kamijo *et al.*, 1998; Weber *et al.*, 1999; Zindy *et al.*, 1998), can both drive apoptosis (Hermeking and Eick, 1994; Wagner *et al.*, 1994; Zindy *et al.*, 1998) and suppress proliferation (Finch *et al.*, 2006). p19^{ARF} may also exert p53-independent tumor suppressive functions (Lowe and Sherr, 2003), in part mediated by

direct binding and functional inactivation of Myc (Datta *et al.*, 2004; Qi *et al.*, 2004). To ascertain whether the low, yet mitogenic, level of deregulated Myc in tissues of $R26^{MER/MER}$ mice is sufficient to induce *ARF* expression, we quantified $p19^{ARF}$ mRNA and protein expression following $MycER^{T2}$ activation (Fig. 4A). Notwithstanding some variability in measured basal levels of *ARF* mRNA between tissues and individual isolates, we saw no measurable induction by Myc of *ARF* mRNA or protein in any tissue except, once again, colonic epithelium. Because it has recently been suggested that even extremely low levels of $p19^{ARF}$ may exert tumor suppressive activity (Bertwistle and Sherr, 2007), we also confirmed genetically that the Myc phenotypes we observe *in vivo* are $p19^{ARF}$-independent by crossing the $R26^{MER/MER}$ mice into the $ARF^{-/-}$ background. *ARF* status had no impact on the extent, kinetics or duration of Myc-induced proliferation in most $R26^{MER/MER}$ mouse tissues (Fig. 4B, C). Together, these data show that the low level of deregulated Myc expressed in most proliferation-permissive tissues of $R26^{MER/MER}$ mice, while adequate to induce widespread proliferation, is insufficient to engage the $p19^{ARF}$/p53 tumor suppressor pathway.

$R26^{MER/MER}$ colonic epithelium was, again, an exception to the above: Myc activation induced a >2 fold induction of *ARF* mRNA (Fig. 4A; P value = 0.004) in colon and induction of $p19^{ARF}$ was confirmed by immunoblotting of colonocyte lysates prepared from fresh tissue (not shown). Furthermore, Myc-induced colonocyte proliferation was significantly enhanced in an $ARF^{-/-}$ background (Fig. 4D). As with apoptosis, this is consistent with the notion that induction of $p19^{ARF}$ requires higher levels of Myc than proliferation.

To ascertain directly whether the thresholds for Myc-induced proliferation versus tumor suppression (induction of apoptosis and *ARF*) are set at different levels of Myc expression *in vivo*, we used the *pIns-*$MycER^{TAM}$ β-cell mouse model in which the powerful rat insulin promoter drives high level expression of 4-OHT-dependent MycER in pancreatic β cells (Suppl. Fig. 5A). We previously showed that activation of Myc in this model efficiently triggers β cell proliferation but that this is rapidly curtailed by concomitant activation of both apoptosis and induction of nucleolar $p19^{ARF}$ (Suppl. Figs. 5A, 5B & 6) (Finch *et al.*, 2006; Pelengaris *et al.*, 2002). Q-PCR and immunoblot analyses of pancreatic islets isolated from *pIns-*$MycER^{TAM}$, $R26^{MER/WT}$ and $R26^{MER/MER}$ mice indicated that $MycER^{TAM}$ mRNA and protein expression are ~15 fold higher in *pIns-*$MycER^{TAM}$ islets than those of $MycER^{T2}$ in islets from homozygous $R26^{MER/MER}$ animals (Fig. 5A and Suppl. Fig. 5C). To compare directly the net outcome of acute Myc activation in *pIns-*$MycER^{TAM}$ versus $Rosa26^{MER/MER}$ islets we activated MycER *in vivo* for 3 and 6 days and then stained pancreatic tissue sections for markers of proliferation (Ki67) and apoptosis (TUNEL). As expected (Finch *et al.*, 2006; Pelengaris *et al.*, 2002), high levels of activated Myc in the *pIns-*$MycER^{TAM}$ islets induced proliferation together with both *ARF* induction and overwhelming β-cell apoptosis, resulting in rapid islet involution. By contrast, activation of low level Myc in islets of $R26^{MER/MER}$ mice drove proliferation without any attendant apoptosis or islet involution, resulting in progressive islet hyperplasia (Fig. 5B and Supp. Fig. 7). Likewise, activation of low-level $MycER^{T2}$ in lung epithelium of $R26^{MER/MER}$ mice failed to elicit *ARF* expression whereas the high levels of $MycER^{T2}$ delivered into lung epithelium by adenovirus vector potently induced *ARF* upon tamoxifen activation (Supp. Fig. 5D). Hence, in both β cells and lung *in vivo*, deregulated Myc is competent to activate intrinsic tumor suppression pathways so long as it is expressed at elevated levels.

There are two plausible explanations for how different threshold levels of Myc might preferentially trigger proliferation versus apoptosis. It could be that low and high levels of Myc engage different sets of target gene sets, perhaps due to differing affinity Myc-binding promoter/enhancer elements (i.e. Myc discriminates) (Suppl. Fig. 8A). In this model, low-level Myc simply fails to activate the apoptotic transcriptional program. Alternatively, Myc might regulate the same genes in each case but to a greater extent when expressed at a higher level,

and the differential Myc outputs arise from different thresholds at which the proliferative and apoptotic programs fire (i.e. downstream factors decide) (Suppl. Fig. 8B). In this case, low level Myc still activates the apoptotic program, but to a level insufficient to trigger it. We reasoned that if the second model holds, sub-apoptotic low-level Myc should, by priming the apoptotic machinery, sensitize cells to induction of apoptosis by other triggers. We therefore co-exposed *R26*$^{MER/MER}$ mice to both tamoxifen, to activate MycER^{T2} in tissues, and a sub-apoptotic dose of the cytotoxic agent doxorubicin. The combination of both sub-apoptotic stimuli triggered significant apoptosis in several tissues, including pancreatic islets and liver, and significantly exacerbated the extent of Myc-induced apoptosis in colonic epithelium (Fig. 6A & B). Thus, low level deregulated Myc, although insufficient to trigger apoptosis itself, nonetheless engages the Myc apoptotic program.

Deregulation of low-level Myc is tumorigenic

Although low-level deregulated Myc is sufficient to drive ectopic proliferation in tissues, it remained possible that actual tumorigenicity, like apoptosis and *ARF* induction, required higher-level Myc expression. To investigate this, we used intranasal delivery of recombinant Adenovirus-expressing Cre (Ad-Cre) to trigger sporadic expression of *MycER*^{T2} in lung epithelia of homozygous *R26*$^{lsl\text{-}MER/lsl\text{-}MER}$ mice. MycER^{T2} was then activated by daily systemic administration of tamoxifen for 3 (n=4) or 6 (n=5) weeks. After 3 weeks of sustained Myc activity, bronchiolar (Fig. 7A, panel 1) and bronchioalevolar junction regions (**panel 2**) of *R26*$^{lsl\text{-}MER/lsl\text{-}MER}$ lungs exhibited multiple hyperplastic and dysplastic epithelial foci with pseudostratification and occasional micropapillary tuft formation. After 6 weeks, more extensive micropapillary and papillary hyperplasia was clearly evident (**panel 3**), with several bronchioles exhibiting Clara cell hyperplasia and sloughing into the airway lumen (**panel 4**). These Myc-induced lesions closely resemble the early bronchiolaveolar lesions that develop 6–8 weeks after sporadic activation of oncogenic *K-Ras*^{G12D} driven from the endogenous *KRas2* promoter (Jackson *et al.*, 2005;Jackson *et al.*, 2001;Johnson *et al.*, 2001).

Individually, Myc or Ras are usually insufficient to drive full tumor progression but together they exhibit potent oncogenic cooperation (Land et al., 1983). To ascertain whether low-level deregulated Myc cooperate with Ras oncogenesis in lung epithelium *in vivo*, we crossed homozygous *R26*$^{lsl\text{-}MER/lsl\text{-}MER}$ and heterozygous *R26*$^{lsl\text{-}MER/wt}$ mice into the conditional *LSL-K-Ras*^{G12D} model (Jackson *et al.*, 2005; Jackson *et al.*, 2001; Johnson *et al.*, 2001). Sporadic co-expression of both oncogenes in lung epithelium was triggered by Ad-Cre, and then MycER^{T2} activated or not with tamoxifen. Induction of *K-Ras*^{G12D} alone elicited atypical adenomatous hyperplasias within 2 weeks, small adenomas by 6 weeks post infection and overt adenocarcinomas only after 16–26 weeks (Jackson *et al.*, 2005; Jackson *et al.*, 2001). Identical hyperplastic and dysplastic bronchiolar lesions arose with identical kinetics and efficiency in *LSL-K-Ras*^{G12D};*R26*$^{lsl\text{-}MER/lsl\text{-}MER}$ mice never given tamoxifen (i.e. where only Ras is activated) (Fig. 7B, panels 1–4) and in control *LSL-K-Ras*^{G12D}-only mice treated with either oil (n=2) or tamoxifen (n=8; data not shown). By contrast, activation of MycER^{T2} *together* with K-Ras^{G12D} profoundly accelerated tumor progression over K-Ras^{G12D} alone in homozygous, but not heterozygous, *Rosa26-lsl-MycER*^{T2} animals. By 6 weeks post Ad-Cre infection, papillary adenomas were both more numerous and significantly larger (**panels 5 and 6**) in co-activated mice, some already having progressed to invasive adenocarcinoma (**panels 9–11**). Such adenocarcinomas were poorly differentiated, growing as small tumor clusters with individual tumor cells embedded within desmoplastic stroma (**panel 10**). Whereas few mitotic figures were evident in the lesions induced by K-Ras^{G12D} alone, they were readily detectable in the bronchiolar lesions (compare **panels 4 and 8**), adenomas (**panel 11**) and adenocarcinomas (**panels 11 and 12**) induced by K-Ras^{G12D} and MycER^{T2} together, indicating that low level expression of deregulated confers a significantly higher level of tumor cell proliferation and is possessed of potent tumorigenic activity.

DISCUSSION

Uncontrolled proliferation of somatic cells is an ever-present risk for large, long-lived organisms like vertebrates whose tissues harbor cells that proliferate throughout life. Hence, multiple surveillance mechanisms have evolved to suppress the emergence and propagation of tumor cells. One of these involves the tight coupling of tumor suppression to the programs that drive cell proliferation, a phenomenon dubbed “intrinsic tumor suppression” (Lowe *et al.*, 2004). Such obligate coupling serves to annul the immediate growth advantage afforded by oncogenic activation of the cell’s proliferative machinery. The Myc transcription factor is a prototypical example of this. In normal cells, Myc coordinates and drives the diverse intra- and extra-cellular programs required for orderly expansion of normal somatic cells. However, oncogenic Myc triggers the ARF/p53 tumor suppressor pathway and apoptosis, two potent tumor suppressor programs that efficiently restrain Myc’s oncogenic potential (Evan and Littlewood, 1998; Lowe *et al.*, 2004). However, for “intrinsic tumor suppression” to be compatible with the orderly proliferation in normal tissues, cells must accurately and reliably discriminate between normal mitogenic and oncogenic signaling. How they do this, however, is unclear. One potential distinctive hallmark of oncogenic signals is their aberrant context: in normal cells Myc is never activated alone but always in the context of collateral signaling pathways. Another possibility is the unusual persistence of oncogenic Myc - endogenous Myc activity is tightly mitogen-dependent and episodic. Finally, as a consequence of its mutation or its relentless induction by other oncogenes, Myc is usually present at significantly higher levels in tumors than in normal cells.

The undeniable importance of intrinsic tumor suppression is demonstrated by the profound acceleration of oncogenesis in Myc transgenic mouse models afforded by genetic lesions that block apoptosis or circumvent the ARF/p53 pathway. Unfortunately, classical transgenic Myc models employ highly active tissue-specific promoter/enhancer elements to drive transgenic Myc expression in the requisite target tissue. Hence, Myc is both deregulated and elevated, making it impossible to ascertain which specific aberrant feature of oncogenic Myc engages tumor suppression. To circumvent this shortcoming, we made use of the relatively weak, but ubiquitous, *Rosa26* promoter to drive low-level deregulated expression of the switchable form of Myc, MycER^{T2}, in target tissues. A MycER^{T2} open reading frame was inserted downstream of the endogenous *Rosa26* promoter but its expression blocked by an intervening transcriptional *STOP* element flanked by *loxP* recombination sites. Hit-and-run excision of the *STOP* element by Cre recombinase triggers targeted expression of MycER^{T2}; however, MycER^{T2} activity is dependent upon continuous provision of 4-OHT ligand.

To ascertain the level at which the *Rosa26* promoter drives MycER^{T2} expression in adult tissues, we crossed mice harboring one or two copies of the *Rosa26-LSL-MycER^{T2}* into the *ZP3*-Cre background, which excises the *floxed* STOP element in the egg. The resulting *R26^{MER}* animals express MycER^{T2} from the *Rosa26* promoter in all tissues. In all tested *R26^{MER}* tissues MycER^{T2} expression levels were broadly comparable, although somewhat higher in colonic epithelium. In every tissue examined, homozygous *R26$^{MER/MER}$* mice expressed approximately twice as much MycER^{T2} mRNA and protein as their heterozygous *R26$^{MER/WT}$* littermates.

Acute activation of MycER^{T2} in tissues of homozygous *R26$^{MER/MER}$* mice triggered widespread ectopic proliferation in many tissues including endocrine and exocrine pancreas, liver, kidney epithelium, lung, skin and lymphoid organs. In most instances, proliferation was sustained at least out to 6 days of continuous Myc activation: analysis beyond this time was curtailed by precipitous onset of anemia and dehydration that coincided with intestinal hemorrhage and necessitated euthanasia. In contrast to homozygous *R26$^{MER/MER}$* mice, activation of MycER^{T2} in heterozygous *R26$^{MER/wt}$* animals elicited no increased proliferation

in any tissues except colon and, weakly, spleen red pulp. Given there is only a two-fold difference in MycER^{T2} levels in heterozygous versus homozygous *R26^{MER}* mice, this defines a sharp minimum threshold level of intracellular Myc required to elicit ectopic proliferation *in vivo*. It also indicates that the level of ectopic activated MycER^{T2} in homozygous *R26$^{MER/MER}$* tissues is close to the minimum necessary to drive ectopic proliferation. It is interesting that the level of ectopic MycER^{T2} in heterozygous *R26$^{MER/WT}$* tissues, while comparable to that of endogenous Myc in MEFs proliferating in response to serum, is insufficient to drive those tissues into cycle. We guess this reflects the fact that serum mitogens co-engage both Myc and multiple, additional synergistic signaling pathways. By contrast, Myc is the sole engine of proliferation in *R26$^{MER/WT}$*cells. It is also possible that activated MycER^{T2} has reduced specific activity compared to *wt* Myc protein, leading to an overestimation of the level of functional Myc in *R26^{MER}* tissues. Of note, while MycER^{T2} was expressed in all *R26$^{MER/MER}$* tissues tested, some failed to proliferate when MycER^{T2} was activated. Why this should be is unclear but it is likely that some cell types are constitutionally unable to proliferate due to structural constraints or lack of critical components of the cell cycle machinery. Yet others may be competent to proliferate only in response to higher levels of Myc than are expressed in *R26$^{MER/MER}$* tissues. An obvious example of this would be those many differentiated cell types that express appreciable levels of Mad proteins (Chin *et al.*, 1995; Queva *et al.*, 1998; Vastrik *et al.*, 1995), which mitigate Myc action by competing with Myc for Max.

Not only is low-level constitutive expression of MycER^{T2} sufficient to induce and maintain aberrant proliferation in many normal *R26$^{MER/MER}$* tissues *in vivo* but it is also oncogenic, efficiently driving early-stage tumorigenesis in lung epithelium and, in cooperation with activated Ras, full progression to invasive adenocarcinoma (Fig. 7). Nonetheless, even though *Rosa26*-driven Myc is oncogenic and both deregulated and active out of normal mitogenic context, it fails to induce either apoptosis or measurable *ARF* expression in most tissue types. This indicates a fundamental difference in how Myc engages its oncogenic and tumor suppressive outputs. The one notable exception to this is colonic epithelium and, since this is the *R26^{MER}* tissue with the highest level of MycER^{T2} expression, we guessed that over-expression of Myc is the likely determining trigger of intrinsic tumor suppression. We confirmed this directly in pancreatic β cells and lung epithelium: in both tissues further elevation of Myc levels triggered both apoptosis and *ARF*. Therefore, we conclude that it is the aberrant intensity of oncogenic Myc, and not its abnormal persistence or context, that triggers intrinsic tumor suppression. Recently it was shown that induction of both *ARF* and replicative senescence by activated Ras *in vivo* also requires over-expression of the activated oncoprotein (Sarkisian *et al.*, 2007). Hence, preternaturally high intensity appears to be the general metric by which cells discriminate between normal and oncogenic signals. However, we do not discount the possibility that even low levels of deregulated Myc may be sufficient, in some cell lineages, to engage apoptosis and/or ARF expression at some level that suppresses tumor initiation. Indeed, data from studies on transgenic Myc in the well-characterized *Eμ-myc* lymphoma model suggest that even very low Myc levels can, at some point in tumor evolution, contribute to the selective pressure to inactivate ARF or p53 (Bertwistle and Sherr, 2007).

Paradoxically, our data suggest that low-level deregulated Myc may be a more efficient initiator of oncogenesis than Myc that is over-expressed, since the latter can be tolerated only by cells that have already lost their tumor suppressor pathways. Indeed, high initial levels of Myc may even impede onset of tumorigenesis, a conclusion consistent with recent surprising findings that co-expression of Myc delays the mean latency of tumor onset in a transgenic *RasG12D* lung tumor model (Tran *et al.*, 2008). This elegant study used the *CC10* promoter to drive Doxycyclin-dependent Myc expression in Clara cells and alveolar type II pneumocytes at very high levels, at least 10 times the quasi-physiological level of MycER^{T2} in lung epithelium of

R26$^{MER/MER}$ mice (Fig. 2A). As our data show, such high levels of Myc breach the *ARF*/apoptotic triggering threshold and, by engaging intrinsic tumor suppression, this has the immediate effect of staunching tumorigenesis. By contrast, oncogenic cooperation in the *LSL-K-Ras*^{G12D};*R26*$^{lsl\text{-}MER/lsl\text{-}MER}$ mouse is efficient because it involves levels of oncogenic Myc (and presumably Ras) that are too low to trigger significant intrinsic tumor suppression. We surmise that low-level oncogene expression may be general characteristic of early stage spontaneous tumors and that most tumors evolve via a two stage selective process. Early on, when tumor suppressor pathways remain intact, selection strongly favors low-level oncogene activity and the relatively indolent clonal expansion it confers. Elevated oncogene activity, together with the increased aggressiveness it confers on tumors, becomes subject to positive selection only once the appropriate intrinsic tumor suppression pathways have been eroded by sporadic mutation.

How might different levels of Myc trigger such distinct biological outputs? One possibility is that Myc-induced *ARF*/p53 and apoptosis are mediated by a distinct set of target genes, perhaps those with lower affinity promoter/enhancer elements that respond only to elevated Myc levels (Supplemental Fig. 5A). Alternatively, Myc might regulate identical sets of gene targets in both cases, although to lesser or greater overall extents when Myc is low or high respectively, with net outcome determined by the different execution thresholds of each output program (Supplemental Fig. 5B). To distinguish between the two possibilities, we asked whether expression of Myc at levels that trigger no overt apoptosis nonetheless reduces the threshold for induction of apoptosis by other insults. MycER^{T2} was globally activated in *R26*$^{MER/MER}$ mice, which were then systemically exposed to the cytotoxic drug Doxorubicin at a dose that was itself sub-apoptotic. The combination of sub-lethal Myc and Doxorubicin induced apoptosis in several tissues. Myc-induced apoptosis is mediated through the intrinsic mitochondrial pathway (Juin *et al.*, 1999) that is triggered when the anti-apoptotic buffering of the Bcl-2/Bcl-x_L proteins is neutralized by the sum of activated BH3 proteins. Our data imply that low-level Myc still activates its requisite BH3 apoptotic effectors but to a level insufficient to neutralize Bcl-2/Bcl-xL without the cooperation of collateral apoptotic signals. Of note, we saw no correlation between Myc-induced proliferation and Myc-induced sensitivity to Doxyrubicin is different tissues, indicating that Myc-dependent Doxyrubicin sensitivity is not merely a consequence of that increased tissue's proliferative status but reflects an inherent variability in the innate sensitivity to Myc-induced apoptosis among different cell types *in vivo*. Indeed, even in any one cell type the threshold for triggering Myc-induced apoptosis is highly dependent upon changes in relative levels of the Bcl-2 family proteins (Bissonnette *et al.*, 1992; Fanidi *et al.*, 1992; Juin *et al.*, 2002; Wagner *et al.*, 1993) and availability of survival signals (Harrington et al., 1994a; Harrington et al., 1994b). Hence, the level of Myc required to trigger apoptosis is not an innate, fixed property of a cell but exquisitely dependent upon the cell's internal state and microenvironment. Importantly, such tissue-specific variations in the threshold set points for Myc oncogenic and apoptotic output mean that the innate susceptibilities of different tissues to Myc-driven oncogenesis will depend greatly on the level at which oncogenic Myc is expressed. Whether the operational threshold at which Myc triggers ARF is similarly subject to such protean, cell type-specific influences is unknown. One last implication of the different firing thresholds at which Myc's distinct outputs (proliferation and tumor suppression) are set is that relatively subtle changes in overall Myc activity may suffice to shift above or below each specific threshold, thereby triggering dramatically different outcomes. Likewise, it is possible that mutations that merely augment or degrade overall Myc activity, by shifting the effective level of Myc above or below different output thresholds, could appear selective for specific Myc functions.

MATERIALS AND METHODS

Generation of *Rosa26-MER* targeting vector and mice

c-*myc* cDNA lacking a stop codon was excised from *pBabe-MycER^{TAM}* (Littlewood *et al.*, 1995) and annealed to T2 point-mutated ligand-binding-domain of human Estrogen Receptor from *pCreER^{T2}* (Indra *et al*., 1999), followed by the *IRES-EGFP* fragment (generously provided by Drs David Dankort and Martin McMahon, UCSF) generating *c-MycER^{T2}-IRES-EGFP* (MIE). This MIE fragment was then incorporated into the previously described *Rosa26* vector *pBigT* (Srinivas *et al*., 2001) then excised incorporating both the floxed *STOP/neomycin^{R}* cassette and *MIE*. The final vector, *pRosa26fsMIE*, was linearized with SwaI, transfected into murine ES cells and Neomycin-resistant clones identified by Southern blotting. An Internal probe was generated by random priming from a gel-purified 1.6 Kb NcoI/HindIII fragment of *pR26-PAS*, further digested with AscI to separate it from co-migrating DNA. External probe was generated by random priming from a 330 bp NotI fragment of the *Rosa26* promoter, generously provided by Dr Philippe Soriano (FHCRC). Chimeric mice were initially bred with *C57/Bl6*, until germ line transmission of the allele was observed. The consequent *R26-lsl-MycER^{T2}* mouse line was bred to *C57/Bl6*, then alternately to *FVBN*, and maintained on a mixed *FVBN/C57/Bl6* background.

Other mouse strains, procedures and genotyping

All procedures involving mice were performed in accordance with protocol number AN 076148 (UCSF IACUC). *Zp3-Cre* (Lewandoski *et al*., 1997), *LSL-K-Ras^{G12D}* (Jackson *et al.*, 2001), *p19$^{ARF-/-}$* (Kamijo *et al.*, 1999) and *pIns-MycER^{TAM}* (Pelengaris *et al.*, 2002) mice are described previously. Tamoxifen (Sigma), dissolved in peanut oil, was administered daily by intraperitoneal (IP) injection for a maximum of 6 weeks at a dose of 1 mg/20 g body mass per day. For BrdU/IdU double labeling, bromodeoxyuridine (Sigma) and Iododeoxyuridine (Sigma), dissolved in Tris buffered saline, were injected IP three times at 6 hr intervals on day 3, while IdU was injected once 5–6 hrs prior to harvest one day after the last tam injection (day 6). To deliver adenovirus-Cre recombinase (Ad-Cre), mice were anesthetized with 2.5% Avertin (250 μl/20 g body mass) and 5×10^7 pfu Ad-Cre was administered as previously described (Fasbender *et al.*, 1998). Details of primer/probe sets used for genotyping and expression analysis can be found in the Supplementary Information.

Cell culture and immunoblotting

Embryonic fibroblasts were isolated from E13.5 *R26-lsl-MycER^{T2}* and *R26-MycER^{T2}* mice. Whole cell lysates were prepared by dissolving cells in Tween lysis buffer [150 mM NaCl; 50 mM HEPES, pH 7.5; 1 mM EDTA; 2.5 mM EGTA; 0.1% Tween 20 + Complete^{TM} protease inhibitor cocktail (PIs; Roche)] followed by sonication. Nuclear extracts were made in low salt buffer [20 mM KCl; 10 mM HEPES, pH 7.5; 1mM MgCl2; 1 mM CaCl2; 0.1% Triton x-100 + PIs]. For liver extracts, freshly isolated livers were homogenized in 10 vol/wt T-Per^{TM} (Pierce) + PIs, fractionated by centrifugation at 1,000 x G and the pellets re-suspended in 1 volume T-Per + 0.2% SDS, followed by sonication. Islets were prepared from disaggregated pancreata as previously described (Lawlor *et al.*, 2006) and lysed in Tween lysis buffer, sonicated and cleared by centrifugation at 12,000 x G prior to loading. For p19^{ARF} analysis, cell lysates were loaded on glycerol/acrylamide gels and fractionated by discontinuous electrophoresis and electroblotted onto PVDF membranes. Anti-ERα (Santa Cruz, SC-543); anti-c-Myc (Santa Cruz, SC42 and 9E10); X-Myc1 (G.E.); anti-p19^{ARF} 5-C3-1 (Bertwistle *et al*., 2004), generously provided by Dr Martine Roussel, St Jude Hospital); anti-Lamin A/C (Santa Cruz, SC7293); anti-α-Actin (Sigma) were used as primary antibodies. Secondary horseradish peroxidase-conjugated antibodies (Amersham) were detected by chemiluminescence.

Immunohistochemistry and immunoflourescence

5 μm paraffin embedded sections were probed with Ki67 antibody (SP6, Neomarkers: Fremont, CA) was used at 1:200 in 3% BSA overnight (o/n) at 4°C and detected with biotinylated goat anti-rabbit (Vector Labs) followed by Vectastain ABC^{TM} detection (Vector Labs) using stable diamobenzidine (DAB) solution (Invitrogen). For BrdU/IdU double staining, mouse α-BrdU (1:20, Roche), which recognizes both BrdU and IdU, was used in conjunction with rat α-BrdU (1:200, Serotec) that recognizes BrdU only. Bound primary antibodies were detected using Alexa-488 conjugated α-mouse IgG and Alexa-568 conjugated α-rat IgG (Molecular Probes). For p19^{ARF} immunohistochemistry, blocking was performed in 10% normal goat serum (NGS) with 0.1% Triton x-100. Primary antibody (5-C3-1) was diluted 1:10 in 3% NGS + 0.1% Triton x-100 and incubated overnight at 4°C. TUNEL staining was performed using the Apoptag^{TM} peroxidase labeled kit (Chemicon) or Apoptag^{TM} flourescein labeled kit (Chemicon) according to the manufacturers directions. Otherwise, tissue sections were blocked overnight in 3% BSA prior to addition of peroxidase-conjugated anti-digoxigenin.

Supplementary Material

Refer to Web version on PubMed Central for supplementary material.

Acknowledgments

We thank all members of the Evan laboratory for sage help in preparing this manuscript, most especially Laura Soucek. Special thanks to Fanya Rostker for animal husbandry. We are grateful to Drs Michael Fried, Martin McMahon, Courtney Broaddus, Doug Hanahan, Kevin Shannon, Doug Green, Francesca Mariani, David Dankort, Suzanne Schubbert, Scott Oakes, Jay Debnath, Scott Kogan and Bill Weiss for insightful comments. We thank all members of the Cancer Center core facilities (Dr. Nigel Kileen, Bill Hyun, Kirsten Copren, Langdon Smythe, Nataliya Korets and Eva Soliven). DJM was supported in part by a Ruth L. Kirschstein NRSA Fellowship (CA099363). MRJ is Enrique Cepero fellow of the Damon Runyon Cancer Research Foundation. Funded by the NIH NCI (R01-CA106526 to GIE).

REFERENCES CITED

Askew DS, Ashmun RA, Simmons BC, Cleveland JL. Constitutive c-*myc* expression in an IL-3-dependent myeloid cell line suppresses cell cycle arrest and accelerates apoptosis. Oncogene 1991;6:1915–1922. [PubMed: 1923514]

Bertwistle D, Sherr CJ. Regulation of the ARF tumor suppressor in *Eμ-Myc* transgenic mice: longitudinal study of Myc-induced lymphomagenesis. Blood 2007;109:792–794. [PubMed: 16968893]

Bertwistle D, Zindy F, Sherr CJ, Roussel MF. Monoclonal antibodies to the mouse p19(Arf) tumor suppressor protein. Hybridomics 2004;23:293–300.

Bissonnette R, Echeverri F, Mahboubi A, Green D. Apoptotic cell death induced by c-*myc* is inhibited by *bcl*-2. Nature 1992;359:552–554. [PubMed: 1406975]

Burns KA, Kuan CY. Low doses of bromo- and iododeoxyuridine produce near-saturation labeling of adult proliferative populations in the dentate gyrus. Eur J Neurosci 2005;21:803–807. [PubMed: 15733099]

Chin L, Schreiber-Agus N, Pellicer I, Chen K, Lee HW, Dudast M, Cordon-Cardo C, DePinho RA. Contrasting roles for Myc and Mad proteins in cellular growth and differentiation. Proc Natl Acad Sci U S A 1995;92:8488–8492. [PubMed: 7667316]

Datta A, Nag A, Pan W, Hay N, Gartel AL, Colamonici O, Mori Y, Raychaudhuri P. Myc-ARF (alternate reading frame) interaction inhibits the functions of Myc. J Biol Chem 2004;279:36698–36707. [PubMed: 15199070]

Eischen CM, Weber JD, Roussel MF, Sherr CJ, Cleveland JL. Disruption of the ARF-Mdm2-p53 tumor suppressor pathway in Myc-induced lymphomagenesis. Genes Dev 1999;13:2658–2669. [PubMed: 10541552]

Evan G, Littlewood T. A matter of life and cell death. Science 1998;281:1317–1322. [PubMed: 9721090]

Evan GI, Wyllie AH, Gilbert CS, Littlewood TD, Land H, Brooks M, Waters CM, Penn LZ, Hancock DC. Induction of apoptosis in fibroblasts by c-myc protein. Cell 1992;69:119–128. [PubMed: 1555236]

Fanidi A, Harrington EA, Evan GI. Cooperative interaction between c-*myc* and *bcl*-2 proto-oncogenes. Nature 1992;359:554–556. [PubMed: 1406976]

Fasbender A, Lee JH, Walters RW, Moninger TO, Zabner J, Welsh MJ. Incorporation of adenovirus in calcium phosphate precipitates enhances gene transfer to airway epithelia in vitro and in vivo. J Clin Invest 1998;102:184–193. [PubMed: 9649572]

Fernandez PC, Frank SR, Wang L, Schroeder M, Liu S, Greene J, Cocito A, Amati B. Genomic targets of the human c-Myc protein. Genes Dev 2003;17:1115–1129. [PubMed: 12695333]

Finch A, Prescott J, Shchors K, Hunt A, Soucek L, Dansen TB, Swigart LB, Evan GI. Bcl-X_L gain of function and $p19^{ARF}$ loss of function cooperate oncogenically with Myc in vivo by distinct mechanisms. Cancer Cell 2006;10:113–120. [PubMed: 16904610]

Flinn EM, Busch CMC, Wright APH. Myc Boxes, which Are conserved in Myc family proteins, are signals for protein degradation via the Proteasome. Mol Cell Biol 1998;18:5961–5969. [PubMed: 9742113]

Harrington EA, Bennett MR, Fanidi A, Evan GI. c-Myc-induced apoptosis in fibroblasts is inhibited by specific cytokines. EMBO J 1994a;13:3286–3295. [PubMed: 8045259]

Harrington EA, Fanidi A, Evan GI. Oncogenes and cell death. Curr Opin Genet Dev 1994b;4:120–129. [PubMed: 8193531]

Hermeking H, Eick D. Mediation of c-Myc-induced apoptosis by p53. Science 1994;265:2091–2093. [PubMed: 8091232]

Indra AK, Warot X, Brocard J, Bornert JM, Xiao JH, Chambon P, Metzger D. Temporally-controlled site-specific mutagenesis in the basal layer of the epidermis: comparison of the recombinase activity of the tamoxifen-inducible Cre-ER(T) and Cre-ER(T2) recombinases. Nucleic Acids Res 1999;27:4324–4327. [PubMed: 10536138]

Jackson EL, Olive KP, Tuveson DA, Bronson R, Crowley D, Brown M, Jacks T. The differential effects of mutant p53 alleles on advanced murine lung cancer. Cancer Res 2005;65:10280–10288. [PubMed: 16288016]

Jackson EL, Willis N, Mercer K, Bronson RT, Crowley D, Montoya R, Jacks T, Tuveson DA. Analysis of lung tumor initiation and progression using conditional expression of oncogenic K-*ras*. Genes Dev 2001;15:3243–3248. [PubMed: 11751630]

Johnson L, Mercer K, Greenbaum D, Bronson RT, Crowley D, Tuveson DA, Jacks T. Somatic activation of the K-*ras* oncogene causes early onset lung cancer in mice. Nature 2001;410:1111–1116. [PubMed: 11323676]

Juin P, Hueber AO, Littlewood T, Evan G. c-Myc-induced sensitization to apoptosis is mediated through cytochrome c release. Genes Dev 1999;13:1367–1381. [PubMed: 10364155]

Juin P, Hunt A, Littlewood T, Griffiths B, Swigart LB, Korsmeyer S, Evan G. c-Myc functionally cooperates with Bax to induce apoptosis. Mol Cell Biol 2002;22:6158–6169. [PubMed: 12167710]

Kamijo T, van de Kamp E, Chong MJ, Zindy F, Diehl JA, Sherr CJ, McKinnon PJ. Loss of the ARF tumor suppressor reverses premature replicative arrest but not radiation hypersensitivity arising from disabled ATM function. Cancer Res 1999;59:2464–2469. [PubMed: 10344759]

Kamijo T, Weber JD, Zambetti G, Zindy F, Roussel MF, Sherr CJ. Functional and physical interactions of the ARF tumor suppressor with p53 and Mdm2. Proc Natl Acad Sci U S A 1998;95:8292–8297. [PubMed: 9653180]

Land H, Parada LF, Weinberg RA. Tumorigenic conversion of primary embryo fibroblasts requires at least two cooperating oncogenes. Nature 1983;304:596–602. [PubMed: 6308472]

Lawlor ER, Soucek L, Brown-Swigart L, Shchors K, Bialucha CU, Evan GI. Reversible kinetic analysis of Myc targets *in vivo* provides novel insights into Myc-mediated tumorigenesis. Cancer Res 2006;66:4591–4601. [PubMed: 16651409]

Lewandoski M, Wassarman KM, Martin GR. *Zp3-cre*, a transgenic mouse line for the activation or inactivation of *loxP*-flanked target genes specifically in the female germ line. Curr Biol 1997;7:148–151. [PubMed: 9016703]

Littlewood TD, Hancock DC, Danielian PS, Parker MG, Evan GI. A modified oestrogen receptor ligand-binding domain as an improved switch for the regulation of heterologous proteins. Nucleic Acids Res 1995;23:1686–1690. [PubMed: 7784172]

Liu J, Levens D. Making myc. Curr Top Microbiol Immunol 2006;302:1–32. [PubMed: 16620023]

Lowe SW, Cepero E, Evan G. Intrinsic tumour suppression. Nature 2004;432:307–315. [PubMed: 15549092]

Lowe SW, Sherr CJ. Tumor suppression by *Ink4a-Arf*: progress and puzzles. Curr Opin Genet Dev 2003;13:77–83. [PubMed: 12573439]

Moore JP, Hancock DC, Littlewood TD, Evan GI. A sensitive and quantitative enzyme-linked immunosorbence assay for the c-*myc* and N-*myc* oncoproteins. Oncogene Res 1987;2:65–80. [PubMed: 3333275]

Nesbit CE, Tersak JM, Prochownik EV. MYC oncogenes and human neoplastic disease. Oncogene 1999;18:3004–3016. [PubMed: 10378696]

Pelengaris S, Khan M, Evan GI. Suppression of Myc-induced apoptosis in beta cells exposes multiple oncogenic properties of Myc and triggers carcinogenic progression. Cell 2002;109:321–334. [PubMed: 12015982]

Penn LJ, Brooks MW, Laufer EM, Land H. Negative autoregulation of c-*myc* transcription. EMBO Journal 1990;9:1113–1121. [PubMed: 2182320]

Popescu NC, Zimonjic DB. Chromosome-mediated alterations of the MYC gene in human cancer. J Cell Mol Med 2002;6:151–159. [PubMed: 12169201]

Qi Y, Gregory MA, Li Z, Brousal JP, West K, Hann SR. p19ARF directly and differentially controls the functions of c-Myc independently of p53. Nature 2004;431:712–717. [PubMed: 15361884]

Queva C, Hurlin PJ, Foley KP, Eisenman RN. Sequential expression of the MAD family of transcriptional repressors during differentiation and development. Oncogene 1998;16:967–977. [PubMed: 9519870]

Rabbitts PH, Watson JV, Lamond A, Forster A, Stinson MA, Evan G, Fischer W, Atherton E, Sheppard R, Rabbitts TH. Metabolism of c-myc gene products: c-myc mRNA and protein expression in the cell cycle. Embo J 1985;4:2009–2015. [PubMed: 4065102]

Ramsay G, Evan GI, Bishop JM. The protein encoded by the human proto-oncogene c-*myc*. Proc Natl Acad Sci USA 1984;81:7742–7746. [PubMed: 6393124]

Sarkisian CJ, Keister BA, Stairs DB, Boxer RB, Moody SE, Chodosh LA. Dose-dependent oncogene-induced senescence *in vivo* and its evasion during mammary tumorigenesis. Nat Cell Biol 2007;9:493–505. [PubMed: 17450133]

Schmitt CA, McCurrach ME, de Stanchina E, Wallace-Brodeur RR, Lowe SW. *INK4a/ARF* mutations accelerate lymphomagenesis and promote chemoresistance by disabling p53. Genes Dev 1999;13:2670–2677. [PubMed: 10541553]

Spencer CA, Groudine M. Control of c-*myc* regulation in normal and neoplastic cells. Adv Cancer Res 1991;56:1–48. [PubMed: 2028839]

Srinivas S, Watanabe T, Lin CS, William CM, Tanabe Y, Jessell TM, Costantini F. Cre reporter strains produced by targeted insertion of EYFP and ECFP into the ROSA26 locus. BMC Dev Biol 2001;1:4. [PubMed: 11299042]

Vastrik I, Kaipainen A, Penttila TL, Lymboussakis A, Alitalo R, Parvinen M, Alitalo K. Expression of the *mad* gene during cell differentiation *in vivo* and its inhibition of cell growth *in vitro*. J Cell Biol 1995;128:1197–1208. [PubMed: 7896882]

Wagner AJ, Kokontis JM, Hay N. Myc-mediated apoptosis requires wild-type p53 in a manner independent of cell cycle arrest and the ability of p53 to induce p21waf1/cip1. Genes Dev 1994;8:2817–2830. [PubMed: 7995520]

Wagner AJ, Small MB, Hay N. Myc-mediated apoptosis is blocked by ectopic expression of *bcl*-2. Mol Cell Biol 1993;13:2432–2440. [PubMed: 8455620]

Weber JD, Taylor LJ, Roussel MF, Sherr CJ, Bar-Sagi D. Nucleolar ARF sequesters Mdm2 and activates p53. Nat Cell Biol 1999;1:20–26. [PubMed: 10559859]

Zindy F, Eischen CM, Randle DH, Kamijo T, Cleveland JL, Sherr CJ, Roussel MF. Myc signaling via the ARF tumor suppressor regulates p53-dependent apoptosis and immortalization. Genes Dev 1998;12:2424–2433. [PubMed: 9694806]

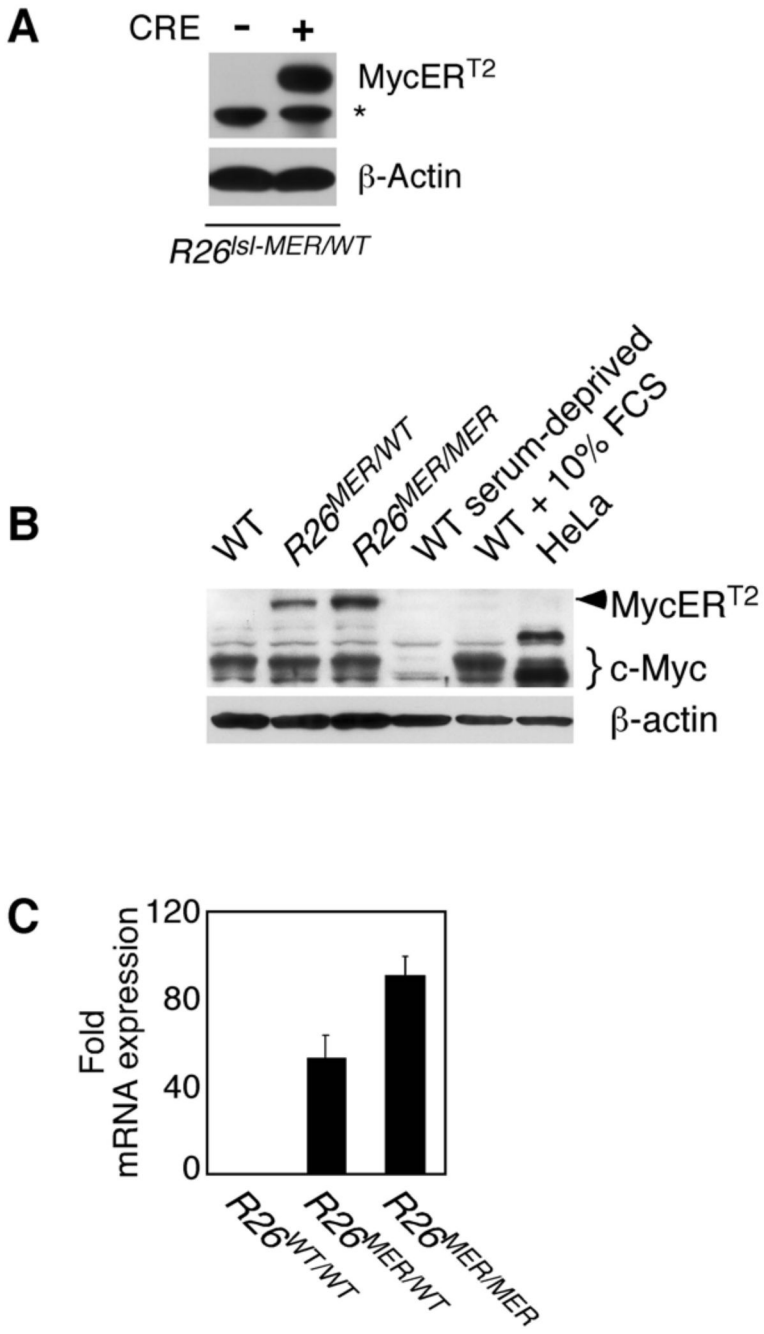

Figure 1. Characteristics of MycER^{T2} expression in *R26$^{lsl\text{-}MER}$* MEFs

A) *Rosa26*-driven MycER^{T2} expression in *R26$^{lsl\text{-}MER}$* MEFs is dependent upon Cre recombinase-dependent and is transgene dose-dependent. *R26$^{lsl\text{-}MER/WT}$* MEFs were infected with retrovirus driving Cre recombinase (+) or control vector (−) and selected with puromycin for 3 days. Western blotting of whole cell lysates with anti-human ERαantibody reveals expression of the predicted 92Kda MycER^{T2} fusion protein. The asterisk denotes a non-specific band.

B) Simultaneous comparison of levels of endogenous Myc and MycER^{T2} in *wt*, *R26$^{MER/wt}$* and *R26$^{MER/MER}$* MEFs. MEFs were isolated from embryos of each genotype and cultured in complete growth medium/10% FBS. Equal numbers of cell equivalents from each lysate were

western blotted with SC42 anti-Myc antibody, detecting an epitope common to endogenous Myc and MycER^{T2}. Extracts from serum-deprived *wt* MEFs and from *wt* MEFs 2 hrs after addition of fresh medium were probed alongside, together with an equivalent number of HeLa cells, which over express c-Myc (~30,000 molecules per cell) for comparison (Moore et al., 1987).

C) Dose dependent expression of *MycER^{T2}* mRNA driven from the *Rosa26* locus. Q-PCR quantitation (mean + SEM) of MycER^{T2} mRNA isolated from in *wt*, *R26$^{MER/WT}$* and *R26$^{MER/MER}$* MEFs, all normalized to *GUS* (n=3).

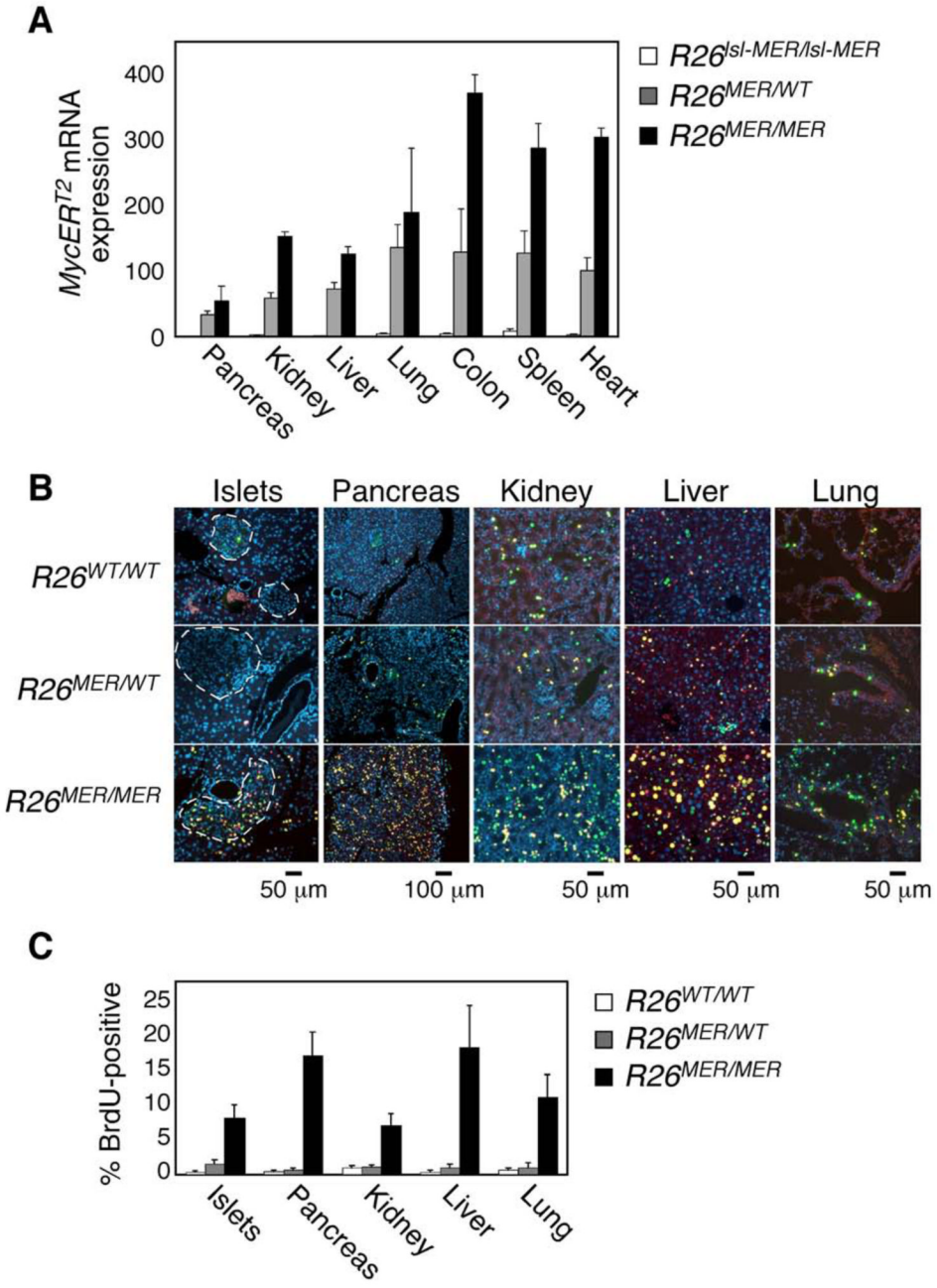

Figure 2. Dose-dependent induction of proliferation by *Rosa26*-driven MycER^{T2} *in* Vivo

A) Q-PCR analysis of MycER^{T2} mRNA levels (mean + SEM) in selected organs from untreated adult *R26$^{lsl-MER/lsl-MER}$* (white bars), *R26$^{MER/WT}$* (grey bars) and *R26$^{MER/MER}$* (black bars) mice, normalized to *GUS* (n=3).

B) Representative images of 2-colour immunofluorescent detection of BrdU/IdU incorporation, indicating instances of S-phase progression in mice treated daily with tamoxifen for 6 days. Yellow-Orange: BrdU incorporation (S phase on day 3); Green: IdU incorporation (S phase on day 6).

C) Quantification (mean + SEM) of BrdU incorporation in tissues of control, *R26$^{MER/wt}$* and *R26$^{MER/MER}$* mice at day 6.

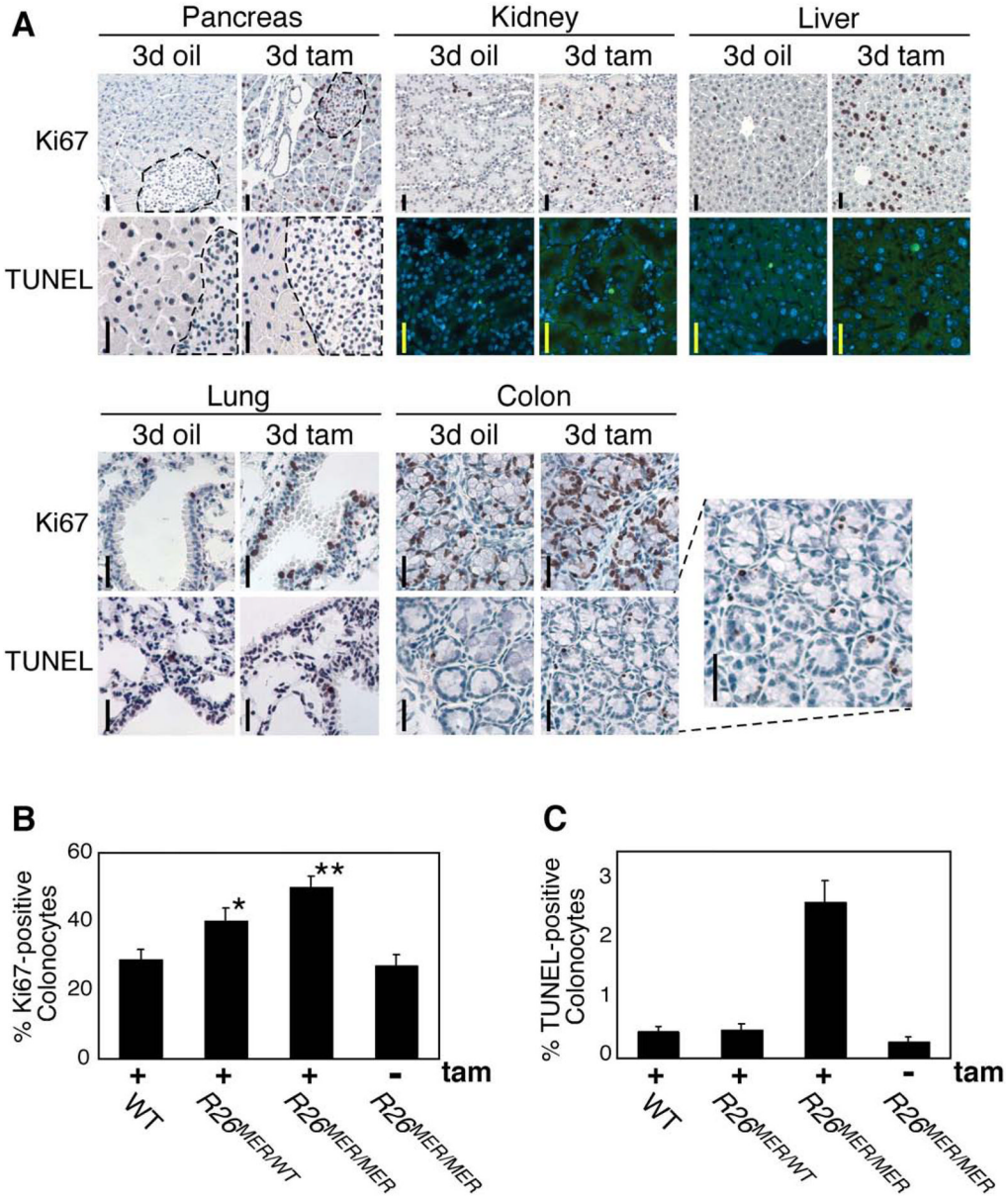

Figure 3. Widespread Myc-induced ectopic proliferation occurs without apoptosis in R26$^{MER/MER}$ mice

A) Organs from adult *R26$^{MER/MER}$* mice treated for 3 days with tamoxifen (tam) (n=7) or oil carrier (n=6), assessed for proliferation (Ki67 staining), and apoptosis (TUNEL assay). Activation of MycER^{T2} drives abundant ectopic cell cycle entry in multiple tissues (exocrine and endocrine pancreas, kidney, liver, lung and colon are presented). However, with the exception of the colon (inset), no tissue exhibited concomitant Myc-induced apoptosis. Scale bars = 25 μm.

B) Quantification (mean + SEM) of Ki67 staining in colon sections from tamoxifen-treated *R26$^{WT/WT}$* (n=4), *R26$^{MER/WT}$* (n=6), *R26$^{MER/MER}$* mice (n=3), and from *R26$^{MER/MER}$* mice treated with carrier (n=3). T Test analysis indicates that the increase in proliferation from *R26$^{WT/WT}$* to *R26$^{MER/WT}$* is significant (* P = 0.001) as is the increase from *R26$^{MER/WT}$* to *R26$^{MER/MER}$* (** P = 0.004).

C) Quantification (mean + SEM) of TUNEL positive cells in sections of colonic epithelium from same mice as B).

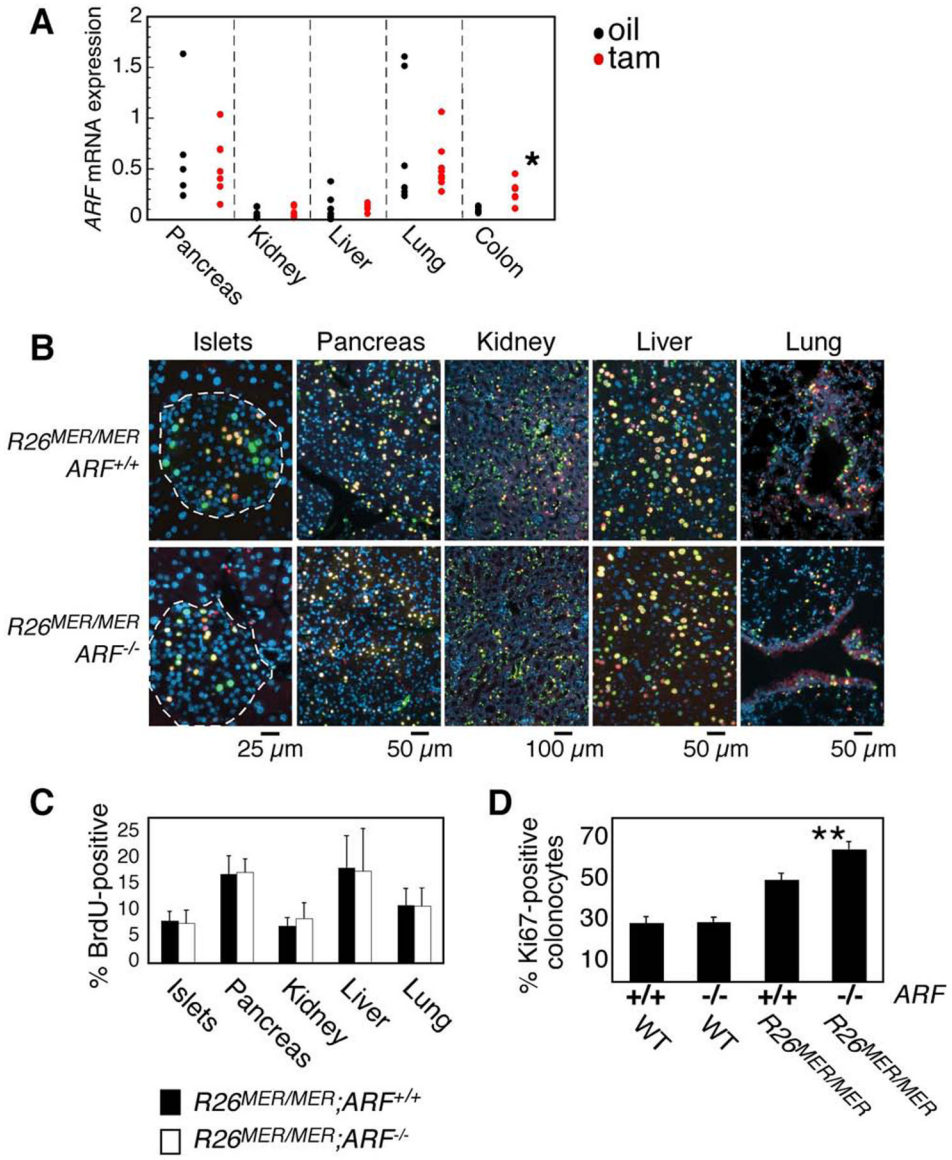

Figure 4. Activation of MycER^{T2} in most tissues of *R26$^{MER/MER}$* does not induce the p19^{ARF} tumor suppressor

A) Q-PCR analysis for expression of *ARF* mRNA in organs from adult *R26$^{MER/MER}$* mice treated for 3 days with tamoxifen (n=7) or oil carrier (n=7), normalized to *GUS*. No *ARF* is induced by MycER^{T2} activation in any tested tissue except for colonic epithelium, where it is statistically significant (* P value = 0.004).

B) Representative 2-colour immunoflourescence images of tissues from *R26$^{MER/MER}$;ARF$^{+/+}$* (n=7) and *R26$^{MER/MER}$;ARF$^{-/-}$* (n=4) mice, injected daily with tamoxifen for 6 days. Mice were systemically pulsed with BrdU on day 2 and IdU on day 6, as per Figure 2, to identify cells in S phase at day 2 (Yellow-Orange) and day 6 (green).

C) Quantification (mean + SEM) of BrdU incorporation on day 6. Note that the data for *ARF$^{+/+}$* are the same as those presented in Figures 2C.

D) Quantification (mean + SEM) of Ki67 staining of colon sections from the indicated mice treated for 3 days with tamoxifen. Data for *ARF$^{+/+}$* samples are the same as those presented in Figure 3B. *R26$^{WT/WT}$;ARF$^{-/-}$* (n=3); *R26$^{MER/MER}$;ARF$^{-/-}$* (n=2).

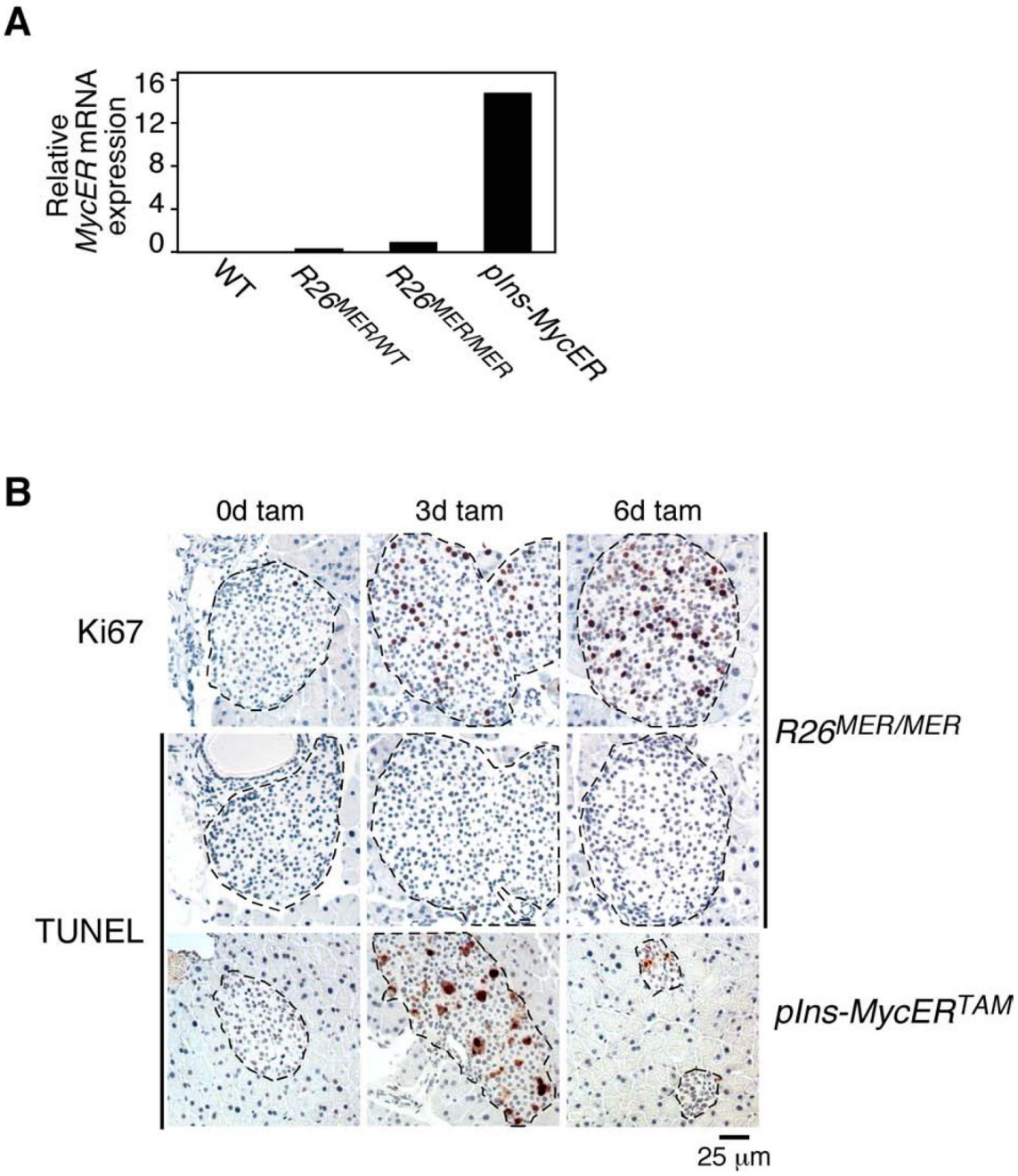

Figure 5. Induction of apoptosis requires higher levels of deregulated Myc than induction of ectopic proliferation

A) Q-PCR analysis of *MycER* mRNA expression in islets isolated from disaggregated pancreata of untreated designated mice, pooled according to genotype (n>2 per cohort). Expression was normalized to *GUS* and results are expressed relative to $MycER^{T2}$ mRNA in $R26^{MER/MER}$ islets.

B) TUNEL staining of pancreatic islets from $R26^{MER/MER}$ mice, treated with tamoxifen for 3 (n=7) or 6 (n=6) days (center panels), with matched samples from similarly treated *pIns-*$MycER^{TAM}$ mice (lower panels). Ki67 staining of adjacent sections from $R26^{MER/MER}$

pancreata (upper panels) demonstrates tamoxifen-induced functionality of *Rosa26*-driven $MycER^{T2}$ protein.

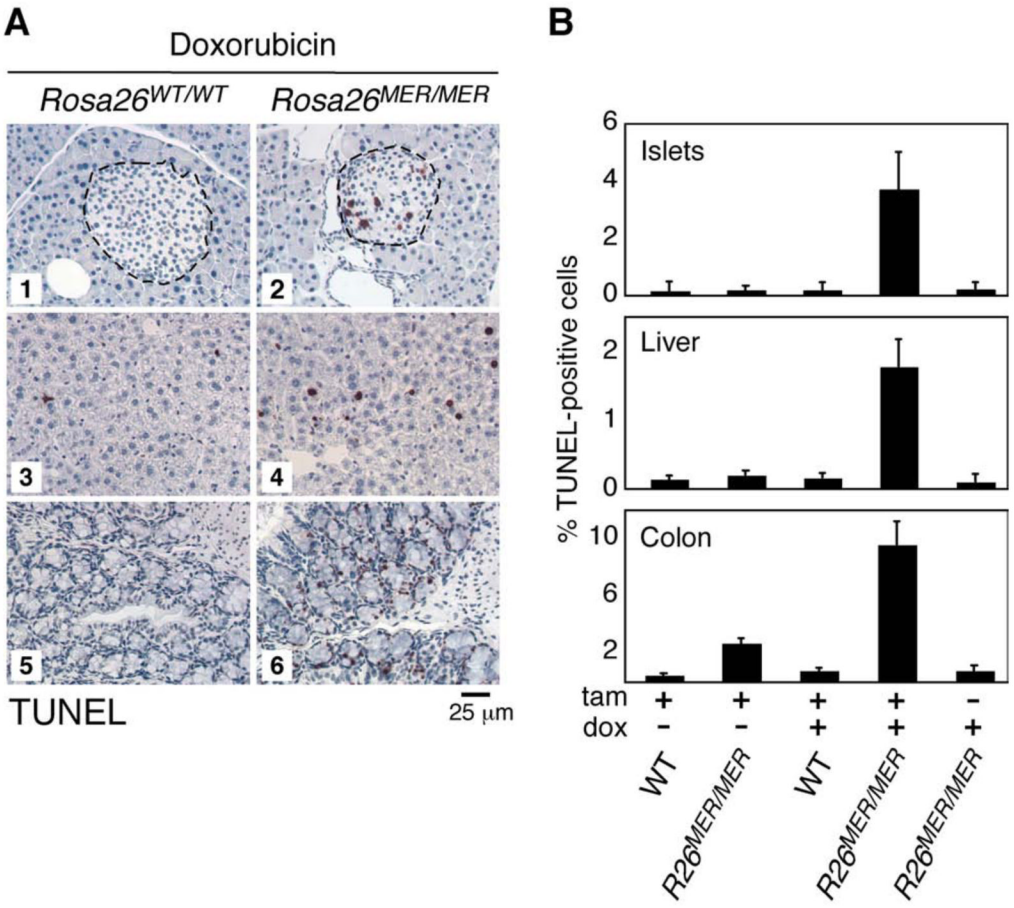

Figure 6. Sub-apoptotic Myc synergises with sub-apoptotic doxorubicin to induce apoptosis in multiple tissues

A) TUNEL staining of pancreatic islets (panels 1, 2), liver (panels 3, 4), and colon (panels 5, 6) from *R26*$^{WT/WT}$ (n=2) and *R26*$^{MER/MER}$ (n=4) mice treated for 3 days with tamoxifen and overnight with 10 mg/kg doxorubicin.

B) Quantification (mean + SEM) of TUNEL staining in sections from pancreas (islets), liver and colon from the above mice treated with tamoxifen and/or doxorubicin. (n=2–4 mice per cohort).

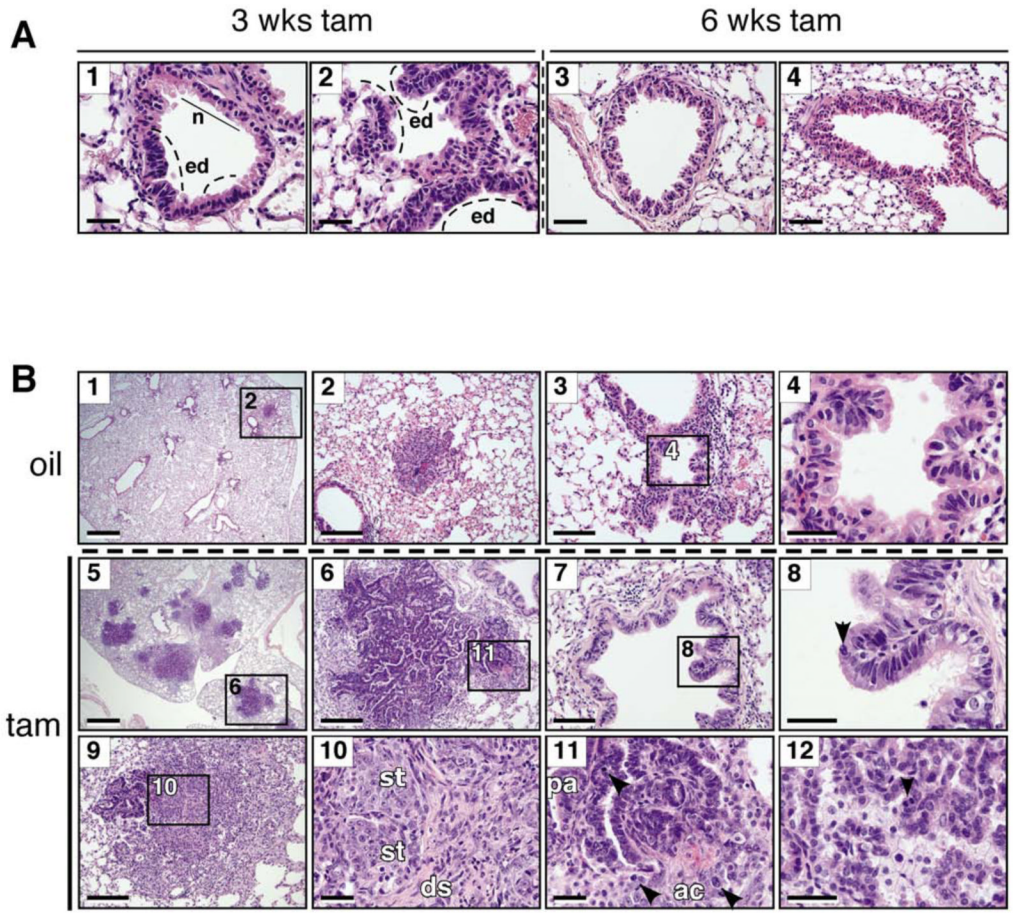

Figure 7. Low level deregulated Myc is tumorigenic *in vivo*

A) Representative images of H & E-stained lungs from tamoxifen treated, Ad-Cre infected *R26*$^{lsl\text{-}MER/lsl\text{-}MER}$ mice showing multiple pre-neoplastic pulmonary lesions. Panels 1, 2: Localized epithelial dysplasia (ed) evident in airway epithelium (panel 1) and bronchioalveolar junctions (panel 2) after 3 weeks of sustained MycER^{T2} activation. Compare with normal bronchiolar epithelium (n). Scale bars=20 μm. Panels 3, 4: Micro-papillary invaginations (panel 3) and atypical Clara cell proliferation characterized by vertical stacking of bronchiolar epithelial cells with apical nuclei (panel 4) present after 6 weeks of sustained MycER^{T2} activation. Scale bars=40 μm.

B) H & E stained lungs from Ad-Cre infected *LSL-K-Ras*^{G12D}*;R26*$^{lsl\text{-}MER/lsl\text{-}MER}$ mice treated with oil carrier (n=3, panels 1–4) or tamoxifen (n=6, panels 5–12) for 6 weeks. Panels 1, 2, 5 & 6: Size comparison between tumors driven by K-Ras^{G12D} alone (1, 2) and K-Ras^{G12D}/MycER^{T2} combined (5, 6). Scale bars=0.4 □m (1, 5) and 100 μm (2, 6). The numbered rectangular regions within panels 1, 3, 5, 6, 7 and 9 are shown enlarged in panels 2, 4, 6, 11, 8, and 10 respectively. Panels 3, 4, 7 & 8: Micropapillary formation along the bronchioles driven by K-Ras^{G12D} alone (3, 4) and K-Ras^{G12D}/MycER^{T2} combined (7, 8). The arrowhead points to a mitotic figure in panel 8. Scale bars=50μm (3, 7) and 20 μm (4, 8). Panels 9–11: Progression to carcinoma observed after 6 weeks of combined Kras^{G12D}/MycER^{T2} driven oncogenesis. Scale bars=100 μm (9) and 20 μm (10, 11, 12). Panel 10: Nests of solid tumor (st) and isolated tumor cells surrounded by desmoplastic stroma (ds). Panels 11, 12: Mitotic figures (arrowheads) present in combined K-Ras^{G12D}/MycER^{T2}-driven papillary adenoma (pa), adenocarcinoma (ac; 11) and acinar adenocarcinoma.